MedChemComm

Accepted Manuscript

This article can be cited before page numbers have been issued, to do this please use: Y. Yu, W. Kuang, R. Huang, Y. Fang, Y. Zhang, Z. Chen and X. Ma, *Med. Chem. Commun.*, 2017, DOI: 10.1039/C7MD00098G.

ROYAL SOCIETY OF CHEMISTRY

rsc.li/medchemcomm

View Article Online
DOI: 10.1039/C7MD00098G

Journal Name

ARTICLE

Design, synthesis and pharmacological evaluation of new 2-oxo-quinoline derivatives containing α-aminophosphonates as potential antitumor agents‡

Received 00th January 20xx,
Accepted 00th January 20xx

DOI: 10.1039/x0xx00000x

www.rsc.org/

Yan-Cheng Yu[a,b,†], Wen-Bin Kuang[b,†], Ri-Zhen Huang[b], Yi-Lin Fang[b], Ye Zhang[a,b,c,*], Zhen-Feng Chen[b,*], Xian-Li Ma[a,*]

A series of novel 2-oxo quinoline derivatives containing α-aminophosphonate were designed and synthesized as antitumor agents. MTT(3-(4, 5-dimethylthiazol-2-yl)-2, 5-diphenyl tetrazolium bromide) assay results demonstrated that some compounds exhibited moderate to high inhibitory activity against HepG2, SK-OV-3 and NCI-H460 cells tumor cell lines, and most compounds showed much lower cytotoxicity against HL-7702 normal cell than 5-FU and cisplatin. The action mechanism of representative compound **5b** was investigated by fluorescence staining assay, flow cytometric analysis and western blot (WB) assay, which indicated that this compound induced apoptosis and involved G_2/M phase arrest accompying by increasing the production of intracellular Ca^{2+} and reactive oxygen species (ROS) and affecting associated enzymes and genes.

1. Introduction

It is well known that cancer is a global health problem and the main causes of mortality worldwide. In order to prevent and combat this disease, a great deal of effort has been devoted to the design and synthesis of new antitumor drugs with high efficiency and low toxicity.

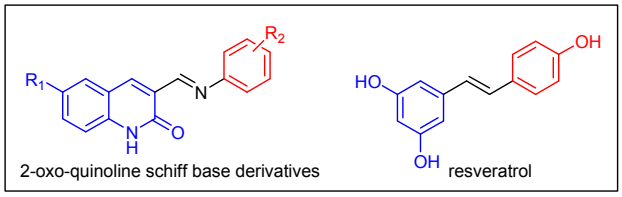

Fig. 1. The chemical structures of 2-oxo-quinoline schiff base derivatives and resveratrol.

Quinoline alkaloids exhibit a variety of outstanding biological activities, including inhibition of cellular proliferation and development changes. So the design and synthesis of new quinoline derivatives with better antitumor activity has attracted many chemists' interest. As the family of quinolines, 2-oxo-quinoline derivatives display potent proliferation inhibitory activity on tumor cells.[1,2] Our previous work has also demonstrated that 2-oxo-quinoline schiff base derivatives exhibited good antioxidant activity and obvious nontoxicity on bald mice.[3,4] In addition, antioxidants are fabricated as the drug candidates to counter these multifarious chronic diseases, containing carcinogenesis, atherogenesis and aging,[5] and many antioxidants exhibit efficient antitumor activity.[6-7] For instance, the powerful antioxidant resveratrol is also deemed as antitumor agents.[7] Moreover, 2-oxo-quinoline schiff base derivatives (Fig. 1) show similar structure with resveratrol and can be considered as its bioisostere derivatives. So it is considered that 2-oxo-quinoline schiff base derivatives may exhibit potent proliferation inhibitory. Furthermore, our previous work has demonstrated that the introduction of aminophosphonate group to pharmacy core is able to increase the antitumor activity and many aminophosphonate derivatives have exhibited potent inhibition activities against human tumors.[8,9] It is thus to expect that the combination of 2-oxo-quinoline schiff base derivatives and aminophosphonate (APA) groups may lead to good antitumor activity and low toxicity. In our previous work, we have described the synthesis, antitumor activity, preliminary apoptosis-inducing and cycle arresting effects of some 2-oxo-quinoline APA derivatives.[10] However, to the best of our knowledge, the scale and mode of the synthesis is still

[a] *College of Pharmacy, Guilin Medical University, Guilin 541004, PR China.*
[b] *State Key Laboratory for the Chemistry and Molecular Engineering of Medicinal Resources (Ministry of Education of China), School of Chemistry and Pharmaceutical Sciences of Guangxi Normal University, Guilin 541004, PR China.*
[c] *Department of Chemistry & Pharmaceutical Science, Guilin Normal College, Guilin 541001, PR China.*
† These authors contributed equally to this work.
‡The authors declare no competing interests.
*Corresponding authors: E-mail address: zhangye81@126.com (Y. Zhang), chenzf@gxnu.edu.cn (Zhen-Feng Chen), mxl78@glmc.edu.cn (Xian-Li Ma). Address: North Ring 2rd Road 109, Guilin 541004, PR China. Tel./Fax.: +86-773-5895132.
Electronic Supplementary Information (ESI) available: ^{1}H NMR, ^{13}C NMR, ESI-MS and crystal data. CCDC No. 1531266, 1531267 and 1531268 for compounds **4c$_5$**, **4d$_2$** and **5c** contain the supplementary crystallographic data for this paper. The data can be obtained free of charge *via* http://www.ccdc.cam.ac.uk, or from the Cambridge Crystallographic Data Centre, 12 Union Road, Cambridge CB21EZ, UK (Fax: (+44) 1223-336-033; E-mail: deposit@ccdc.cam.ac.uk). See DOI: 10.1039/x0xx00000x.

View Article Online
DOI: 10.1039/C7MD00098G

limited. Particularly, the cytotoxicity on normal cells(i.e., toxicity), the further apoptosis-inducing and cycle arresting mechanism of 2-oxo-quinoline schiff base derivatives with APA moieties has not been reported. Therefore, in the present work, as a continuation of our previous work, we introduced some APA moiety to different 2-oxo-quinoline schiff base skeleton and evaluated the *in vitro* cytotoxicity of the target compounds. Moreover, the mechanism of apoptosis and cycle arrest was further deeply and systematically investigated.

2. Results and discussion

2.1. Chemistry

2-Oxo-quinoline derivatives bearing APA moiety (compounds **4** and **5**) were synthesized as shown in Scheme 1. Firstly, 2-chloro-quinoline-3-carbaldehyde derivatives **2**(**2a-2d**) were obtained via Vilsmeier-Haack-Arnold reaction according to our previous work,[3] which included the condensation of acetanilide derivatives **1**(**1a-1d**) with N,N-dimethylformamide (DMF) in the presence of phosphorusoxychloride. 2-Oxo-quinoline 3-carbaldehyde derivatives **3**(**3a-3d**) were then obtained in good yields by the hydrolytic reaction of **2**(**2a-2d**) in the presence of 70% acetic acid aqueous solution.[3] The target compounds **4**(**4a$_1$-4d$_7$**) were synthesized by the Kabachnik-Fields reaction, which executed by the simultaneous condensation of compounds **3**, diethyl phosphate and many kinds of amines, through a one-pot three-component synthesis method. The other target compounds **5**(**5a-5d**) were also synthesized by the condensation of compounds **3** with diethyl 4-aminobenzylphosphonate. The structures of target compounds **4**(**4a$_1$-4d$_7$**) and **5**(**5a-5d**), were confirmed using various spectroscopic methods, including ^{1}H NMR, ^{13}C NMR and high-resolution mass spectrometry (HR-MS)(Part 3 of supplementary data). In order to better understand the structures of these target compounds, the crystal structures of compounds **4c$_5$**, **4d$_2$** and **5c** were also determined by X-ray diffraction (Fig. 2, selected relevant parameters see in part 1 of supplementary data). As shown in Fig. 2, the crystals structure of compounds **4c$_5$**, **4d$_2$** and **5c** were well consistent with the characterization data of NMR and HR-MS, indirectly confirming the structures of target compounds **4**-**5**.

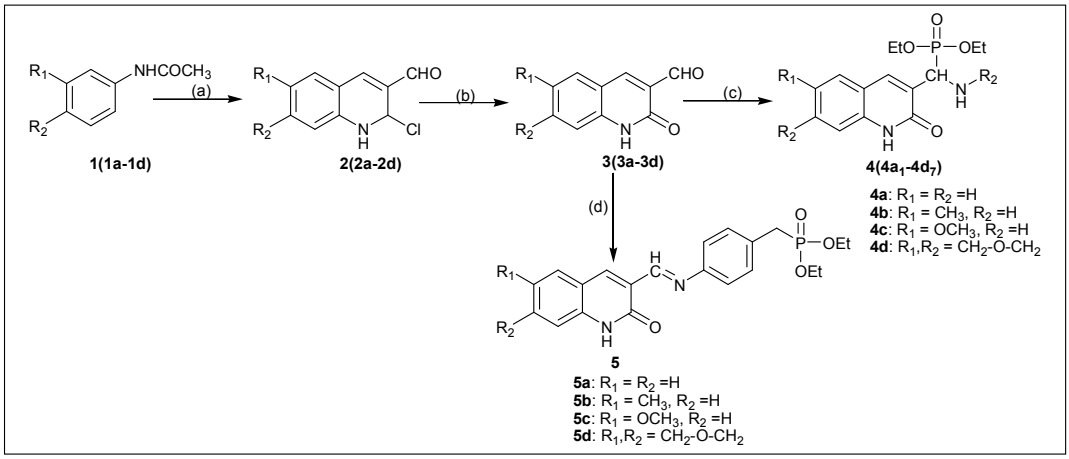

Scheme 1. General synthetic route for compound **3–5**. Reagents and conditions: (a) $POCl_3$/DMF; (b) 70% acetic acid aqueous solution; (c) diethyl phosphite, amines, CH_3CN; (d) diethyl 4-aminobenzylphosphonate, CH_3CN.

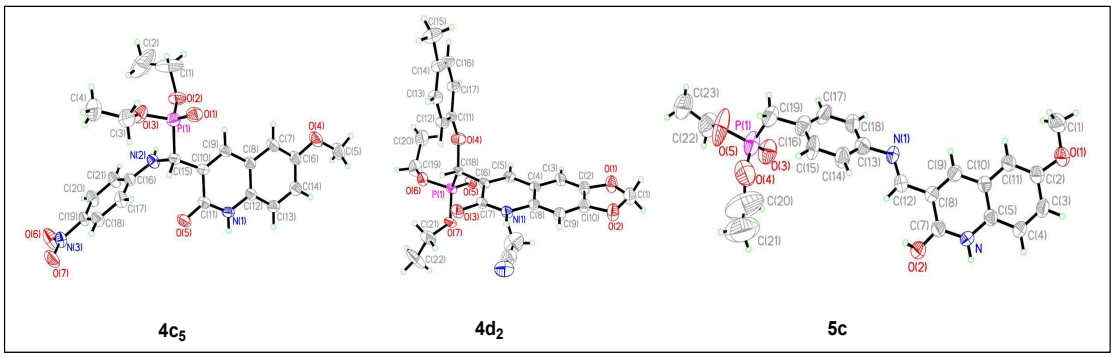

Fig. 2. The crystal structures of compounds **4c$_5$**, **4d$_2$** and **5c**.

2.2 Biological Activity

2.2.1 Cytotoxicity Test

The *in vitro* cytoxicity of the compounds **4**(**4a$_1$-4d$_7$**) and **5**(**5a-5d**) were evaluated by methylthiazoltetrazolium (MTT)

View Article Online
DOI: 10.1039/C7MD00098G

assay against HepG2 (Human liver cancer cell line), SK-OV-3 (human ovarian cancer cell line), NCI-H460 (Human large cell lung cancer cell line) and HL-7702 (Human liver normal cell line) cell lines. Two commercial anticancer drugs 5-fluorouracil (5-FU) and cisplatin were used as positive controls. The results were shown in Table 1.

As shown in Table 1, most of target compounds **4–5** displayed much higher inhibitory activity than their corresponding 2-oxo-quinoline 3-carbaldehyde derivatives **3**(**3a–3d**) against the HepG2, SKOV3 and NCI-H460 cell lines, indicating the introduction of α-aminophosphonates on 2-oxo-quinoline may improve the antitumor activity. It was important to note that some target compounds showed better cytotoxic inhibition against these three cell lines than 5-FU, while they displayed lower cytotoxicity on HL-7702 normal cell line than that of commercial anticancer drugs 5-fluorouracil (5-FU) and cisplatin, indicating that they may be good candidate for anti-tumour drugs. Table 1 also demonstrated that, for compound **4**, both of the substituents (R_1) in 2-oxo-quinoline group and the substituents (R_2) in α-aminophosphonates moiety had important influence on the cytotoxic inhibition, though the influence was irregular. In addition, by the comparasion of cytotoxic inhibition activity of compounds **4** and **5**, it could be also concluded that the schiff base bond had potent effect on the antitumor activity.

In HepG2 assay, compounds **4c$_5$**, **5a**, **5b**, **5c** and **5d** exhibited better cytotoxicity than the commercial anticancer drug 5-FU (IC_{50}=31.98 μM), with IC_{50} of 20.80 μM, 17.85 μM, 9.99 μM, 17.31 μM and 28.92 μM, respectively. It was worth noting that compound **5b** even exhibited better cytotoxic inhibition than cisplatin (IC_{50}=10.12 μM), implying its favourable inhibition activities of on HepG2 cell line. So compound **5b** was then selected as representative compound to assay the action mechanism of these 2-oxo-quinoline APA derivatives **4-5**.

In SKOV-3 assay, compounds **4a$_7$**, **4c$_5$**, **4d$_6$** and **4d$_7$** displayed better cytotoxicity than 5-FU (IC_{50}=26.34 μM), with IC_{50} of 25.81μM, 25.13μM, 26.25μM and 22.36 μM, respectively. It was obvious that compound **4d$_7$** showed the best cytotoxic inhibition among these compounds. Pity of it was that no compound exhibited better cytotoxic inhibition than cisplatin in this cell line.

In NCI-H460 assay, compounds **4c$_5$** and **5b** exhibited better cytotoxic inhibition than 5-FU (IC_{50}=45.44 μM), with IC_{50} of 44.56 and 38.96μM, respectively, while these was no compound demonstrated better cytotoxic inhibition than cisplatin in this assay.

Table 1. [α]IC_{50} values of 2-oxo-quinoline derivatives bearing APA moiety (**4**-**5**) towards three selected tumor cell lines and normal cell line for 48 h.

Compounds	IC_{50}(μM)			
	HepG2	SKOV-3	NCI-H460	HL-7702
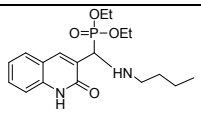 **4a$_1$**	61.43±2.14	38.30±1.74	>100	>100
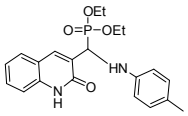 **4a$_2$**	67.27±2.35	66.75±2.48	>100	>100
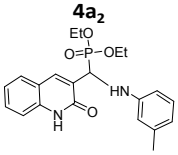 **4a$_3$**	65.46±2.64	55.95±1.11	>100	>100
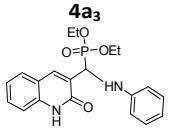 **4a$_4$**	46.33±2.02	54.11±1.18	>100	>100
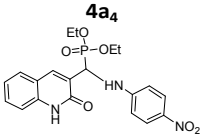 **4a$_5$**	75.21±3.74	29.98±0.91	>100	>100
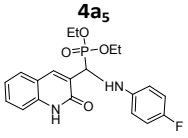 **4a$_6$**	37.21±2.23	40.95±0.85	>100	>100

View Article Online
DOI: 10.1039/C7MD00098G

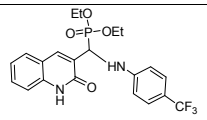 **4a$_7$**	39.12±2.11	25.81±0.54	>100	>100
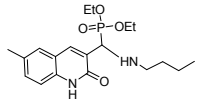 **4b$_1$**	39.17±3.12	130.26±4.59	>100	>100
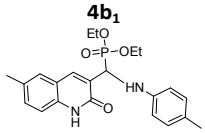 **4b$_2$**	37.57±1.45	37.22±1.34	>100	>100
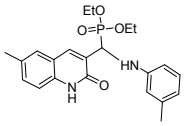 **4b$_3$**	45.95±1.78	342.40±4.26	>100	>100
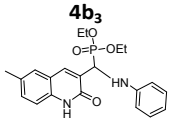 **4b$_4$**	39.56±1.54	69.37±1.08	>100	>100
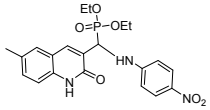 **4b$_5$**	35.61±2.73	>200	>100	>100
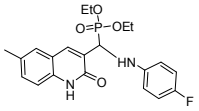 **4b$_6$**	46.21±2.11	30.33±0.66	>100	>100
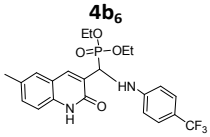 **4b$_7$**	68.11±2.64	191.26±4.02	>100	>100
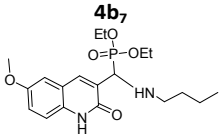 **4c$_1$**	43.25±3.35	58.21±1.75	>100	>100
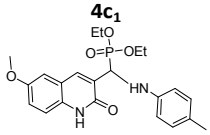 **4c$_2$**	57.63±2.75	59.96±2.77	>100	>100
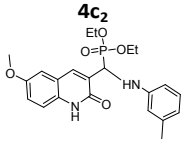 **4c$_3$**	45.54±2.85	73.011±2.29	>100	>100
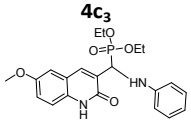 **4c$_4$**	60.77±3.01	54.66±1.95	>100	>100

View Article Online
DOI: 10.1039/C7MD00098G

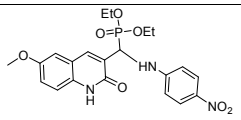 **4c$_5$**	20.80±1.65	25.13±1.04	44.56±2.56	>100
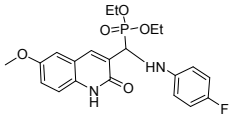 **4c$_6$**	58.92±2.27	269.696±5.12	>100	>100
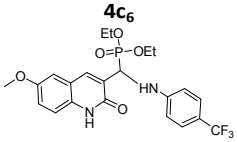 **4c$_7$**	40.15±1.88	102.11±4.39	>100	>100
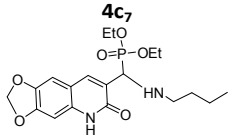 **4d$_1$**	46.27±2.66	37.23±1.95	47.86±2.05	>100
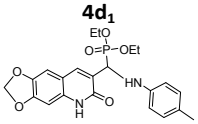 **4d$_2$**	43.11±1.17	48.89±1.53	>100	>100
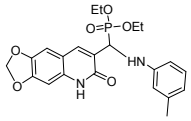 **4d$_3$**	>100	>100	>100	>100
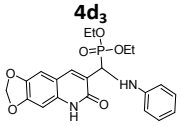 **4d$_4$**	45.21±3.14	64.95±2.43	>100	>100
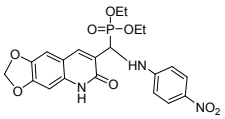 **4d$_5$**	44.01±1.31	28.23±0.75	>100	>100
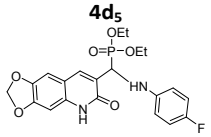 **4d$_6$**	37.95±1.98	26.25±0.87	59.56±2.75	>100
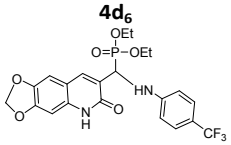 **4d7**	78.95±4.45	22.36±0.45	>100	>100
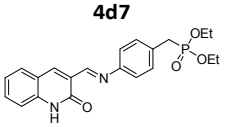 **5a**	17.85±0.68	35.97±0.98	57.88±2.24	>100
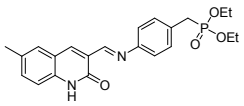 **5b**	9.99±0.25	34.76±1.14	38.96±1.88	>100

View Article Online
DOI: 10.1039/C7MD00098G

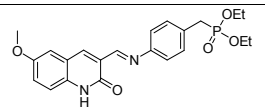 **5c**	17.31±1.13	52.991±1.61	>100	>100
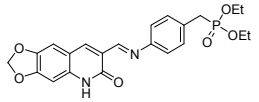 **5d**	28.92±1.47	47.92±1.14	>100	>100
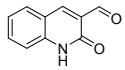 **3a**	>200	>200	>200	>100
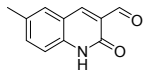 **3b**	>200	>200	>200	>100
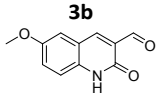 **3c**	>200	>200	>200	>100
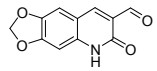 **3d**	>200	>200	>200	>100
5-FU	31.98±0.56	26.34±0.57	45.44±0.94	58.74±2.31
Cis-platin	10.12±0.71	15.60± 1.70	20.36±0.50	15.67±0.32

[α]IC_{50} values are presented as the mean ± SD (standard error of the mean) from three separated experiments.

2.2.2. Investigation of Cell Cycle Distribution

Cell cycle checkpoints are significant control mechanisms that ensure the nonreversible performance of cell cycle events.[11] Understanding of cell cycle distribution may provide important information to the regulation of the cell cycle.[12] To determine the possible role of cell cycle arrest in 2-oxo-quinoline APA derivatives induced growth inhibition, HepG2 cells were treated with the representative compound **5b** at different concentrations (0, 8, 10 and 12 μM) for 48 h. As shown in Fig. 3, treating of HepG2 cells with compound **5b** increased cell cycle arrest at the G_2 phase, leading to a significant increase in the G_2-phase population (34.68%(8μM), 36.92%(10μM) and 46.77%(12μM)) compared with the control cells (19.04%). The G_1-phase and S-phase population of HepG2 cells reduced by 35.31%(8μM), 33.91%(10μM), 25.75%(12μM) and 30.01%(8μM), 29.16%(10μM), 27.49%(12μM), respectively, compared with that of control (50.47% and 30.49%). The results evidently demonstrated that compound **5b** potentially arrested the cell cycle of HepG2 cells in the G_2/M stage in a concentration-dependent manner.

G_2/M transition is basically mediated by timed activation of distinct cyclin B1/CDK1(CDC2) complexes which is mainly regulated by the positive regulator CDC25C phosphatase.[12,13] CDC25C dephosphorylates CDK1 resulting to the activation of cyclin B1/CDK1 complex and performance of G_2/M transition.[12,13] In response to DNA damage or other alteration causing to G_2/M arrest, phosphorylation of CDC25C results to its degradation and sequestration in the cytoplasm, which eventually leads to the destabilization of cyclin-CDK complexes.[14] Moreover, the anti-oncogene p53, p27 and p21 protein also plays a significant role in G_2/M arrest through promoting accumulation of the inactive cyclin B-CDK complex, by which lead to the regulation to G_2/M transition.[15]. So the expression of these regulatory proteins including cyclin B1, CDK1 and CDC25C, as well as p53, p27 and p21 anti-oncogenes, were further evaluated by western blot assay, using glyceraldehyde-3-phosphate dehydrogenase (GAPDH) as control. As shown in Fig.4, the HepG2 cell lysates demonstrated that compound **5b** dramatically decreased the expression of cyclin B1, CDK1 and CDC25C in a dose-dependent manner, accompanied by a dose-dependent increase in the level of p53, p21 and p27 protein compared with controls. These results clearly displayed that compounds **5b** potentially induced G_2/M phase cell cycle arrest in HepG2 cells, which might be one of the reasons for its antiproliferative effect.

2.2.3. Apoptosis Assay study by mitochondrial membrane potential staining

Apoptosis is a key pathway leading to cell death and has been considered as another effective approach in cancer treatment.[16] Its assays may provide important information for preliminary investigation of the mode of action.[16-19] So it may be interested to investigate the apoptosis-inducing effect of compound **5b**. In order to investigate the apoptosis-inducing effect of target compound **5b**, mitochondrial membrane potential changes were designed and detected, using the fluorescent probe JC-1. HepG2 cells treated with compound **5b** at 10 μM for 12 h were stained with JC-1 and not treated with the compound **5b** were used as control. The results were shown in Fig. 5. For fluorescence microscopy, Fig. 5 showed that cells not treated with the compound **5b** were normally red, while for compound **5b** treatment, cells showed strong

View Article Online
DOI: 10.1039/C7MD00098G

green fluorescence and indicated typical apoptotic morphology after 12 h. The phenomenon suggested that compound **5b** was able to induce apoptotic cell morphology in HepG2 cell line.[17-19]

2.2.4. Apoptosis Assay study by Hoechst 33258 Staining

The apoptosis-inducing effect of compound **5b** was also determined by Hoechst 33258 staining of HepG2 cancer cells and the result were shown in Fig. 6. As shown in Fig. 6, HepG2 cells not treated with compound **5b** were normally stained as blue, while treated with **5b** for 12 h showed strong blue fluorescence and had characteristic apoptotic morphologies. The observations demonstrated that compound **5b** induced apoptosis of HepG2 cells, consistent with that of previous experiment of mitochondrial membrane potential staining.

2.2.5. Apoptosis Assay study by Acridine Orange/Ethidium Bromide (AO/EB) Staining

To further characterize the cell apoptosis induced by compound **5b**, AO/EB staining was performed to evaluate the accompanying changes in morphology. The cytotoxicity of compound **5b** was evaluated in HepG2 cells following treatment with 10 μM for 24 h. HepG2 cells not treated with **5b** were used as control. The results (Fig. 7) showed that the morphology of **5b**-treated HepG2 cells had changed significantly. The cell nuclei were stained yellow green or orange, and the morphology showed pycnosis, membrane blebbing and cell budding characteristic of apoptosis. These phenomena were associated with cell apoptosis, indicating that compound **5b** was able to induce the apoptosis of HepG2 cells.

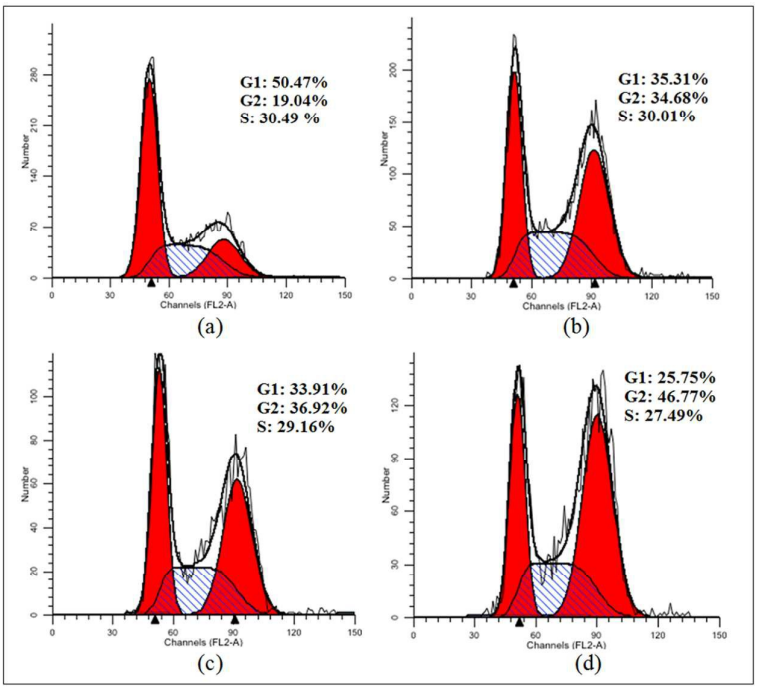

Fig. 3. Cell cycle analysis of compound **5b** treated with HepG2 cells. HepG2 cells were treated with different concentrations compound **5d** ((a) 0μM, (b) 8μM, (c) 10μM and (d) 12μM) for 48 h to determine cell cycle phase distribution.

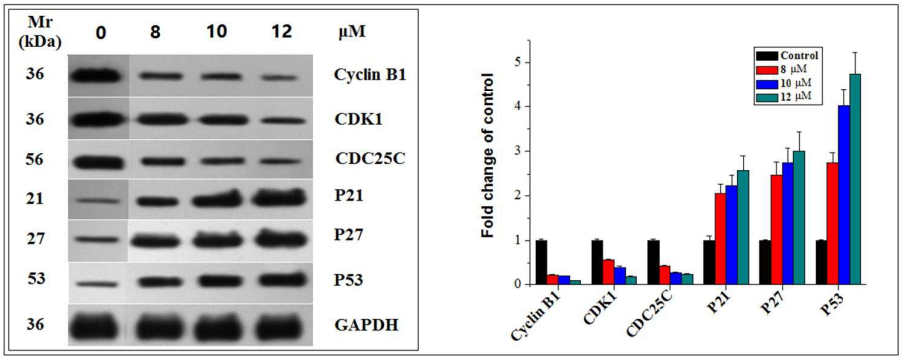

Fig. 4. Effect of compound **5b** on the expression of cyclins and associated proteins. HepG2 cells were treated with compound **5b** for 48 h. Western blot analysis was carried out with antibodies against cyclin B1, CDK1, CDC25C and *GAPDH* was used as loading control.

View Article Online
DOI: 10.1039/C7MD00098G

Journal Name

ARTICLE

2.2.6. Apoptosis Assay study by Flow Cytometry

The apoptosis ratios induced by compound **5b** in HepG2 tumor cells were quantitatively assayed by flow cytometry and the result was shown in Fig. 8. The result contained the differentiation of live cells (annexin V^-/PI^-), early apoptotic cells (annexin V^+/PI^-), late apoptotic cells (annexin V^+/PI^+), and necrotic cells (annexin V^-/PI^+). Treating of HepG2 cells with different concentration (8, 10 and 12 μM) compound **5b** led to the increment of apoptotic cells population, from 8.41% in controls to 34.57%(i.e., 15.49% early apoptotic cells and 19.08% late apoptotic cells) (8 μM), 43.62%(i.e., 9.24% early apoptotic cells and 34.38% late apoptotic cells) (10 μM) and 54.90%(i.e., 15.49% early apoptotic cells and 19.08% late apoptotic cells) (12 μM) in treated cells (i.e., 11.83% early apoptotic cells and 43.07% late apoptotic cells). The results demonstrated that the apoptosis of HepG2 cells treated with compound **5b** increased gradually with concentration and compound **5b** may suppress cell proliferation by inducing apoptosis.

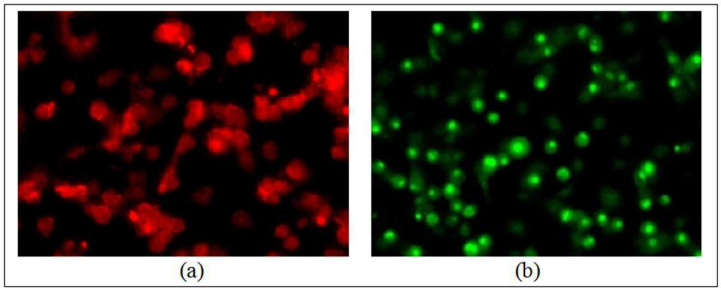

Fig. 5. Mitochondrial membrane potential staining of compound **5b** on HepG2 cells. (a) The cells not treated with **5b** were used as control, (b) compound **5b** treated HepG2 cells at concentration of 10 μM, respectively.

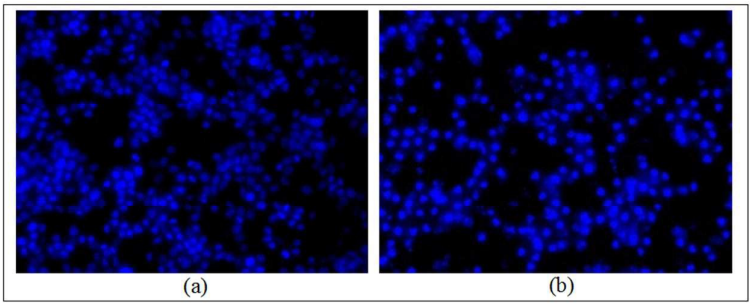

Fig. 6. Effects of compound **5b** on morphological changes of HepG2 cells after staining with Hoechst 33258 dye. (a) The cells not treated with **5b** were used as control, (b) compound **5b** treated HepG2 cells at concentrations of 10 μM, respectively.

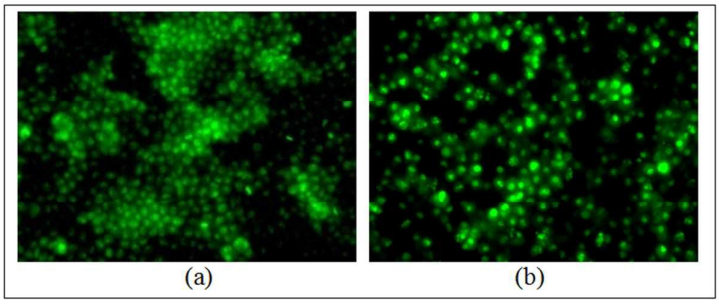

View Article Online
DOI: 10.1039/C7MD00098G

Fig. 7. Compound **5b** induced apoptosis in HepG2 cells were determined by AO/EB staining and were photographed via fluorescence microscopy. (a) Not dealt with compound **5b** was used as control at for 24 h, (b) dealt with compound **5b** for 24 h at concentrations of 10 μM, respectively.

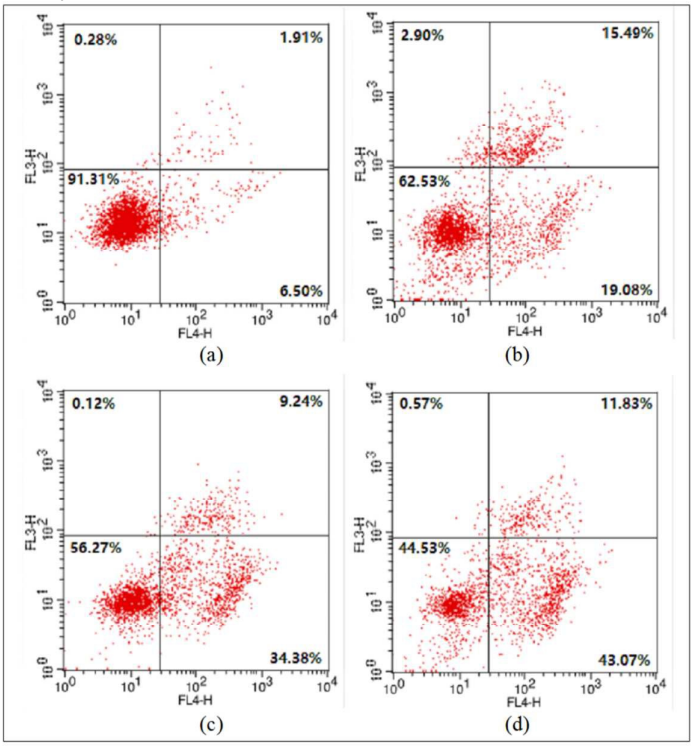

Figure 8. Apoptosis ratio detection of compound **5b** (b) 8μM, (c) 10μM, (d) 12μM) against HepG2 cells by Annexin V/PI assay and the control (a) was used as comparation.

2.2.7. ROS generation assay

Previous work has proved that the generation of intracellular reactive oxygen species (ROS) may lead to the induction of apoptosis.[20,21] To investigate the role of ROS in **5b**-induced apoptosis in HepG2 cells, the ROS levels was investigated by fluorescence microscopy using 4',6-diamidino-2-phenylindole dihydrochloride (**DAPI**) and 2,7-dichlorofluorescein diacetate (**DCFH-DA**) as fluorescent probe. As shown in Fig. 9, for **DAPI** staining, HepG2 cells treated with compound **5b** displayed more strong fluorescence in the cytoplasm, while the control that untreated control cells was weak and spread over the cells. For **DCFH-DA** staining, HepG2 cells treated with compound **5b** exhibited stronger green fluorescence**,** indicating that **5b** significantly up-regulated generation of ROS and induced apoptosis of HepG2 cells. The phenomenon indicated that compounds **5b** significantly increased the intracellular level of ROS and was generally considered as cues for the induction of apoptosis.[17-19]

2.2.8. Intracellular Ca^{2+} Release

Intracellular calcium played important role in inducing cell apoptosis and the overload of intracellular calcium can induce cell apoptosis.[22,23] Our above results have demonstrated that compound **5b** can induce apoptosis of HepG2 cells. To determine the role of calcium signaling in **5b**-induced apoptosis, HepG2 cells were treated with **5b** for 24 h and Ca^{2+} was synchronously detected by fluorescence microscopy with a calcium indicator dye **DCFH-DA** (Fig. 10). As shown in Fig. 10, treatment with **5b** led to an increment of Ca^{2+} in the HepG2 cells. The results implied that **5b**-induced apoptosis might be associated with its induction of Ca^{2+} increment.

2.2.9. Caspase-dependent Apoptosis in HepG2 Cells

As a physiological program of cellular death, apoptosis plays a vital role during normal development and in cellular homeostasis. It is well-known that Both Fas-dependent and mitochondria-dependent apoptotic pathways are considered as major pathways directly causing neuronal apoptosis, which are associated with expression of Bax, Bcl-2 and cytochrome *c* proteins.[24,25] To test the mechanism of **5b**-induced apoptosis in HepG2 cells, the expression of Bax, Bcl-2 and cytochrome *c* was also investigated by western blotting assay. As shown in Fig. 11, treatment of HepG2 cells with **5b** resulted to an elevation in the expression of Bax and reduction in expression of Bcl-2 accompanied by the release of mitochondrial cytochrome *c* into the cytosol. The results suggested that **5b** induced apoptosis by regulating the levels of Bcl-2 family proteins, Bax and Bcl-2.

Caspases are a family of cysteinyl aspartate specific proteases contained in apoptosis and are dichotomized to groups of initiators (caspases 8, 9 and 10) and executioners (caspases 3, 6 and 7).[19] The caspase cascade, which is initiated by the proteolysis of inactive procaspases, is propagated by

View Article Online
DOI: 10.1039/C7MD00098G

the cleavage of downstream caspases and substrates such as poly (ADP-ribose) polymerase cleavage (PARP). To determine whether caspases were activated in **5b**-induced apoptosis, the expression of caspase-9, -3 and PARP was investigated by western blot assay (Fig. 11). As shown in Fig. 11, HepG2 cells treated with compound **5b** led to a significant increment in the expression of caspase-9, -3 and PARP compared to control. These results indicated that compound **5b** might induce apoptosis through a mitochondrial mediated pathway and caspase cascade.

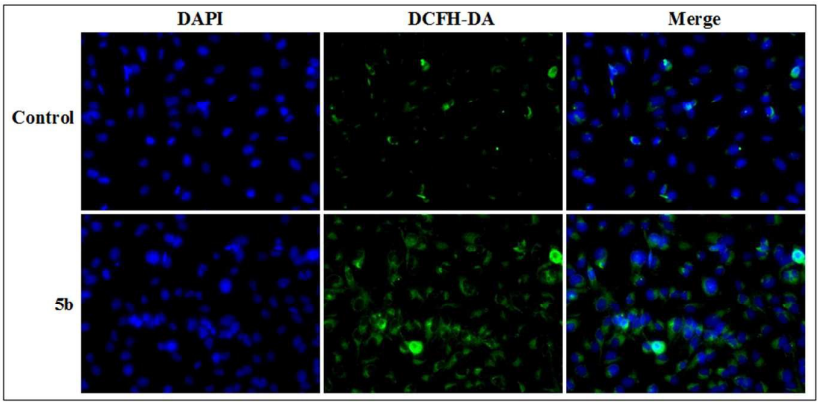

Fig. 9. Compound **5b** (10μM) affected the levels of intracellular ROS in HepG2 cells.

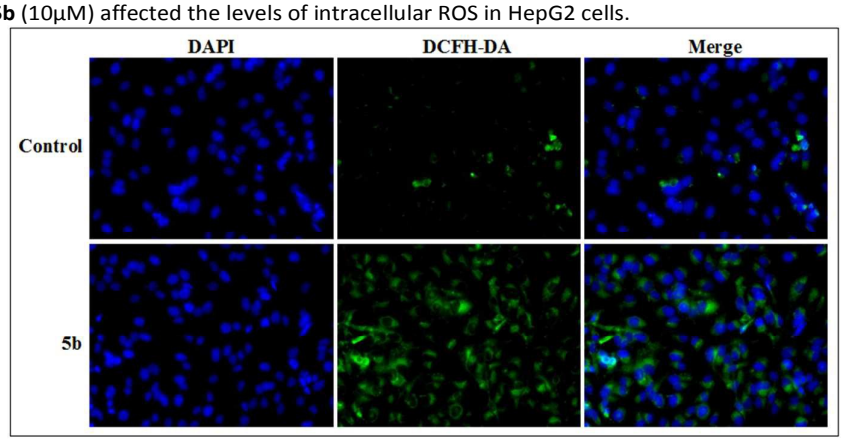

Fig. 10. Compound **5b** (10μM) caused the levels of intracellular Ca^{2+} elevation in HepG2 cells.

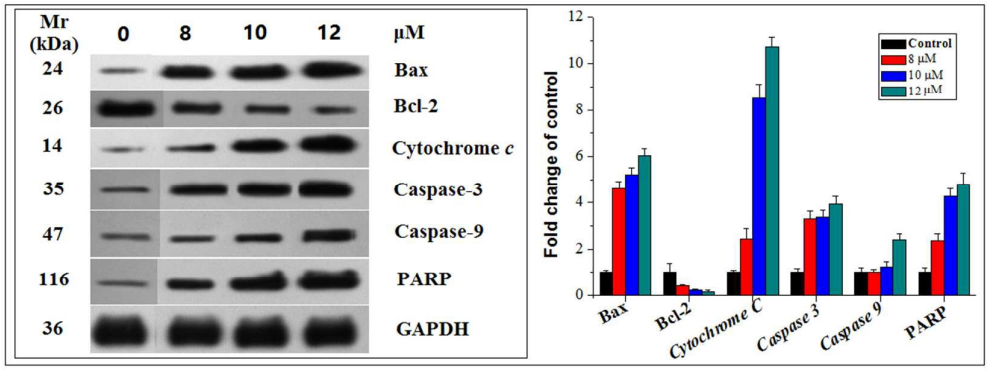

Fig. 11. Effects of compound **5b** on the level of cytochrome *c*, Bcl-2, Bax, Caspase-9, Caspase-3 and p53. HepG2 cells were treated with of compound **5b** for 24 h at different concentrations. Equal amount of protein was loaded on SDS-PAGE gel for western blot analysis as described in experimental section. Glyceraldehyde-3-phosphate dehydrogenase(GAPDH) was used as an internal control.

3. Experimental Section

3.1. Chemistry

All chemicals (reagent grade) were commercially available and used without further purification. NMR spectra were

View Article Online
DOI: 10.1039/C7MD00098G

assayed on a BRUKER AVANCE AV500 spectrometer using tetramethyl silane, (TMS) as the internal standard. The mass spectra were determined on a BRUKER ESQUIRE HCT spectrometer. GelRed nucleic acid stain was purchased from Biotium.

3.1.1 General procedure for compound 4(4a$_1$-4d$_7$)

2-oxo-quinoline 3-carbaldehyde derivatives **3** (1 mmol), primarily amines (1.5 mmol), diethyl phosphate (1mmol) and 3 mL acetonitrile were mixed in pressure tube and reacted at 105^{o}C for 4h. After the reaction, the mixture was cooled to room temperature and filtered to yield compound **4** as white or yellow powder.

4a$_1$: Yield54.29%, ^{1}H NMR (500 MHz, DMSO) δ 11.87 (s, 1H), 8.05 (d, *J* = 3.7 Hz, 1H), 7.65 (d, *J* = 7.7 Hz, 1H), 7.49 (t, *J* = 7.7 Hz, 1H), 7.31 (d, *J* = 8.2 Hz, 1H), 7.19 (t, *J* = 7.5 Hz, 1H), 4.48 (d, *J* = 21.9 Hz, 1H), 4.14 – 4.05 (m, 2H), 3.96 – 3.84 (m, 2H), 2.40 (ddd, *J* = 25.7, 13.6, 7.0 Hz, 2H), 1.36 (dt, *J* = 14.0, 7.0 Hz, 2H), 1.26 (ddd, *J* = 16.7, 10.7, 5.3 Hz, 5H), 1.08 (t, *J* = 7.0 Hz, 3H), 0.82 (t, *J* = 7.3 Hz, 3H).^{13}C NMR (126 MHz, DMSO) δ 161.98, 161.93, 138.40, 137.70, 137.64, 130.60, 129.88, 128.18, 122.42, 119.55, 119.53, 115.37, 62.92, 62.87, 62.42, 62.36, 53.20, 51.96, 47.67, 47.55, 40.48, 40.31, 40.23, 40.14, 39.98, 39.81, 39.64, 39.48, 31.86, 20.17, 16.79, 16.74, 16.63, 16.58, 14.26.ESI-HRMS *m/z* Calc for $C_{18}H_{27}N_2O_4P$ $[M+H]^+$:367.1787; found: 367.1782.

4a$_2$: Yield75.82%, ^{1}H NMR (500 MHz, DMSO) δ 11.96 (s, 1H), 8.08 (d, *J* = 3.7 Hz, 1H), 7.57 (d, *J* = 7.7 Hz, 1H), 7.48 (t, *J* = 7.6 Hz, 1H), 7.31 (d, *J* = 8.2 Hz, 1H), 7.19 – 7.14 (m, 1H), 6.85 (d, *J* = 8.3 Hz, 2H), 6.62 (d, *J* = 8.5 Hz, 2H), 6.11 (dd, *J* = 10.4, 6.2 Hz, 1H), 5.26 (dd, *J* = 24.5, 10.4 Hz, 1H), 4.11 (dq, *J* = 14.2, 7.1 Hz, 2H), 4.02 – 3.87 (m, 2H), 2.09 (s, 3H), 1.22 (t, *J* = 7.1 Hz, 3H), 1.08 (t, *J* = 7.0 Hz, 3H).^{13}C NMR (126 MHz, DMSO) δ 161.68, 161.64, 145.11, 144.99, 138.47, 137.65, 137.60, 130.80, 130.13, 129.78, 128.12, 126.32, 122.56, 119.40, 119.38, 115.50, 113.86, 63.22, 63.16, 62.92, 62.86, 48.28, 47.05, 40.50, 40.43, 40.34, 40.26, 40.17, 40.00, 39.84, 39.67, 39.50, 20.45, 16.77, 16.73, 16.58, 16.54.ESI-HRMS *m/z* Calc for $C_{21}H_{25}N_2O_4P$ $[M+Na]^+$:423.1450; found: 423.1447.

4a$_3$: Yield70.24%, ^{1}H NMR (400 MHz, DMSO) δ 12.00 (s, 1H), 8.10 (d, *J* = 3.7 Hz, 1H), 7.59 (d, *J* = 7.7 Hz, 1H), 7.48 (t, *J* = 7.7 Hz, 1H), 7.31 (d, *J* = 8.2 Hz, 1H), 7.17 (t, *J* = 7.5 Hz, 1H), 6.93 (t, *J* = 7.8 Hz, 1H), 6.57 (s, 1H), 6.50 (d, *J* = 8.1 Hz, 1H), 6.39 (d, *J* = 7.4 Hz, 1H), 6.25 (dd, *J* = 10.2, 6.2 Hz, 1H), 5.30 (dd, *J* = 24.4, 10.3 Hz, 1H), 4.12 (dq, *J* = 14.2, 7.1 Hz, 2H), 4.04 – 3.85 (m, 2H), 2.13 (s, 3H), 1.22 (t, *J* = 7.1 Hz, 3H), 1.09 (t, *J* = 7.0 Hz, 3H).^{13}C NMR (101 MHz, DMSO) δ 161.66, 161.61, 147.46, 147.32, 138.46, 138.35, 137.73, 137.67, 130.86, 130.14, 129.24, 128.16, 122.60, 119.39, 119.36, 118.69, 115.51, 114.43, 110.74, 63.26, 63.19, 62.97, 62.90, 48.02, 46.47, 40.57, 40.36, 40.15, 39.95, 39.74, 39.53, 39.32, 21.78, 16.79, 16.73, 16.60, 16.54. ESI-HRMS *m/z* Calc for $C_{21}H_{25}N_2O_4P$ $[M-H]^-$:399.1474; found: 399.1493.

4a$_4$: Yield63.62%, ^{1}H NMR (500 MHz, DMSO) δ 11.87 (s, 1H), 8.05 (d, J = 3.7 Hz, 1H), 7.65 (d, J = 7.7 Hz, 1H), 7.49 (t, J = 7.7 Hz, 1H), 7.31 (d, J = 8.2 Hz, 1H), 7.19 (t, J = 7.5 Hz, 1H), 4.48 (d, J = 21.9 Hz, 1H), 4.14 – 4.05 (m, 2H), 3.96 – 3.84 (m, 2H), 2.40 (ddd, J = 25.7, 13.6, 7.0 Hz, 2H), 1.36 (dt, J = 14.0, 7.0 Hz, 2H), 1.26 (ddd, J = 16.7, 10.7, 5.3 Hz, 5H), 1.08 (t, J = 7.0 Hz, 3H), 0.82 (t, J = 7.3 Hz, 3H).^{13}C NMR (126 MHz, DMSO) δ 161.66, 161.62, 147.44, 147.33, 138.48, 137.76, 137.71, 130.87, 129.99, 129.36, 128.16, 122.60, 119.39, 119.36, 117.79, 115.53, 113.65, 63.26, 63.21, 62.99, 62.93, 47.97, 46.73, 40.47, 40.30, 40.14, 39.97, 39.80, 39.63, 39.47, 16.76, 16.72, 16.58, 16.53.ESI-HRMS *m/z* Calc for $C_{20}H_{23}N_2O_4P$ $[M+Na]^+$:409.1293; found: 409.1293.

4a$_5$: Yield73.01%, ^{1}H NMR (400 MHz, DMSO) δ 12.13 (s, 1H), 8.13 (d, J = 3.4 Hz, 1H), 8.03 (d, J = 9.3 Hz, 2H), 7.95 (dd, J = 9.4, 5.6 Hz, 1H), 7.66 (d, J = 7.7 Hz, 1H), 7.54 (t, J = 7.5 Hz, 1H), 7.35 (d, J = 8.2 Hz, 1H), 7.25 – 7.17 (m, 1H), 6.86 (d, J = 9.3 Hz, 2H), 5.47 (dd, J = 22.6, 9.4 Hz, 1H), 4.21 – 3.88 (m, 4H), 1.21 (t, J = 7.0 Hz, 3H), 1.11 (t, J = 7.0 Hz, 3H)^{13}C NMR (101 MHz, DMSO) δ 161.37, 161.31, 153.69, 153.58, 138.63, 138.45, 138.39, 137.66, 131.28, 128.59, 128.41, 126.45, 122.77, 119.18, 119.15, 115.65, 112.43, 63.46, 63.39, 63.36, 63.29, 47.73, 46.17, 40.60, 40.39, 40.18, 39.98, 39.77, 39.56, 39.35, 16.78, 16.72, 16.59, 16.54. ESI-HRMS *m/z* Calc for $C_{20}H_{22}N_3O_6P$ $[M+Na]^+$:454.1144; found: 454.1163.

4a$_6$: Yield79.13%, ^{1}H NMR (400 MHz, DMSO) δ 12.00 (s, 1H), 8.10 (d, *J* = 3.7 Hz, 1H), 7.59 (d, *J* = 7.7 Hz, 1H), 7.50 (t, *J* = 7.7 Hz, 1H), 7.32 (d, *J* = 8.2 Hz, 1H), 7.22 – 7.14 (m, 1H), 6.96 – 6.85 (m, 2H), 6.71 (ddd, *J* = 6.8, 5.2, 2.8 Hz, 2H), 6.37 (dd, *J* = 10.3, 6.3 Hz, 1H), 5.25 (dd, *J* = 24.4, 10.3 Hz, 1H), 4.13 (dq, *J* = 14.2, 7.1 Hz, 2H), 4.05 – 3.84 (m, 2H), 1.23 (t, *J* = 7.0 Hz, 3H), 1.09 (t, *J* = 7.0 Hz, 3H).^{13}C NMR (101 MHz, DMSO) δ 161.68, 161.62, 156.67, 154.36, 144.10, 143.95, 138.49, 137.78, 137.71, 130.92, 129.82, 128.19, 122.62, 119.35, 119.31, 115.88, 115.66, 115.54, 114.60, 114.53, 63.27, 63.20, 62.99, 62.92, 48.53, 46.98, 40.60, 40.39, 40.19, 39.98, 39.77, 39.56, 39.35, 16.79, 16.74, 16.59, 16.54.ESI-HRMS *m/z* Calc for $C_{20}H_{22}FN_2O_4P$ $[M+Na]^+$:427.1199; found: 427.1204.

4a$_7$: Yield80.64%, ^{1}H NMR (400 MHz, DMSO) δ 12.13 (s, 1H), 8.13 (d, *J* = 3.4 Hz, 1H), 8.03 (d, *J* = 9.3 Hz, 2H), 7.95 (dd, *J* = 9.4, 5.6 Hz, 1H), 7.66 (d, *J* = 7.7 Hz, 1H), 7.54 (t, *J* = 7.5 Hz, 1H), 7.35 (d, *J* = 8.2 Hz, 1H), 7.25 – 7.17 (m, 1H), 6.86 (d, *J* = 9.3 Hz, 2H), 5.47 (dd, *J* = 22.6, 9.4 Hz, 1H), 4.21 – 3.88 (m, 4H), 1.21 (t, *J* = 7.0 Hz, 3H), 1.11 (t, *J* = 7.0 Hz, 3H).^{13}C NMR (101 MHz, DMSO) δ 161.52, 161.47, 150.77, 150.64, 138.56, 138.03, 137.97, 131.07, 129.29, 128.28, 126.88, 126.75, 126.71, 124.19, 122.68, 119.27, 119.24, 117.62, 117.30, 115.59, 112.99, 99.99, 63.35, 63.29, 63.16, 63.09, 47.66, 46.10, 40.60, 40.39, 40.18, 39.97, 39.76, 39.56, 39.35, 16.76, 16.71, 16.59, 16.53.ESI-HRMS *m/z* Calc for $C_{21}H_{22}F_3N_2O_4P$ $[M+Na]^+$: 477.1167; found: 477.1165.

4b$_1$: Yield38.61%, ^{1}H NMR (500 MHz, DMSO) δ 11.87 (s, 1H), 8.05 (d, *J* = 3.7 Hz, 1H), 7.65 (d, *J* = 7.7 Hz, 1H), 7.49 (t, *J* = 7.7 Hz, 1H), 7.31 (d, *J* = 8.2 Hz, 1H), 7.19 (t, *J* = 7.5 Hz, 1H), 4.48 (d, *J* = 21.9 Hz, 1H), 4.14 – 4.05 (m, 2H), 3.96 – 3.84 (m, 2H), 2.40 (ddd, *J* = 25.7, 13.6, 7.0 Hz, 2H), 1.36 (dt, *J* = 14.0, 7.0 Hz, 2H), 1.26 (ddd, *J* = 16.7, 10.7, 5.3 Hz, 5H), 1.08 (t, *J* = 7.0 Hz, 3H), 0.82 (t, *J* = 7.3 Hz, 3H).^{13}C NMR (126 MHz, DMSO) δ 161.86, 161.82, 137.44, 137.39, 136.41, 131.83, 131.39, 129.77, 127.65, 119.50, 119.47, 115.29, 62.87, 62.82, 62.39, 62.34, 53.21, 51.97, 47.65, 47.53, 40.52, 40.35, 40.18, 40.02, 39.85,

View Article Online
DOI: 10.1039/C7MD00098G

39.68, 39.52, 31.85, 20.83, 20.18, 16.80, 16.76, 16.64, 16.60, 14.28.ESI-HRMS *m/z* Calc for $C_{19}H_{29}N_2O_4P$ $[M+H]^+$: 381.1943; found: 381.1953.

4b$_2$: Yield75.87%, ^{1}H NMR (400 MHz, DMSO) δ 11.88 (s, 1H), 8.01 (d, *J* = 3.6 Hz, 1H), 7.38 – 7.27 (m, 2H), 7.21 (d, *J* = 8.3 Hz, 1H), 6.85 (d, *J* = 8.2 Hz, 2H), 6.61 (d, *J* = 8.3 Hz, 2H), 6.12 (dd, *J* = 10.4, 6.2 Hz, 1H), 5.26 (dd, *J* = 24.5, 10.5 Hz, 1H), 4.11 (p, *J* = 7.2 Hz, 2H), 4.02 – 3.82 (m, 2H), 2.31 (s, 3H), 2.08 (s, 3H), 1.22 (t, *J* = 7.0 Hz, 3H), 1.07 (t, *J* = 7.0 Hz, 3H). ^{13}C NMR (101 MHz, DMSO) δ 161.58, 161.53, 145.14, 144.99, 137.44, 137.37, 136.46, 132.05, 131.60, 129.99, 129.76, 127.57, 126.27, 119.35, 119.32, 115.39, 113.87, 63.20, 63.13, 62.93, 62.86, 48.37, 46.82, 40.59, 40.38, 40.17, 39.96, 39.75, 39.54, 39.34, 20.78, 20.46, 16.79, 16.74, 16.60, 16.54.ESI-HRMS *m/z* Calc for $C_{22}H_{27}N_2O_4P$ $[M+Na]^+$:437.1606; found: 437.1616.

4b$_3$: Yield71.80%, ^{1}H NMR (500 MHz, DMSO) δ 11.89 (s, 1H), 8.02 (d, *J* = 3.7 Hz, 1H), 7.36 (s, 1H), 7.31 (d, *J* = 8.4 Hz, 1H), 7.21 (d, *J* = 8.4 Hz, 1H), 6.92 (t, *J* = 7.8 Hz, 1H), 6.56 (s, 1H), 6.49 (dd, *J* = 8.1, 1.8 Hz, 1H), 6.39 (d, *J* = 7.4 Hz, 1H), 6.21 (dd, *J* = 10.3, 6.2 Hz, 1H), 5.29 (dd, *J* = 24.4, 10.3 Hz, 1H), 4.12 – 3.86 (m, 4H), 2.31 (s, 3H), 2.13 (s, 3H), 1.25 (t, *J* = 7.1 Hz, 1H), 1.21 (d, *J* = 7.0 Hz, 3H), 1.08 (t, *J* = 7.0 Hz, 3H).^{13}C NMR (126 MHz, DMSO) δ 161.55, 161.51, 147.46, 147.35, 138.32, 137.49, 137.44, 136.47, 132.06, 131.62, 130.00, 129.20, 127.60, 119.36, 119.34, 118.66, 115.41, 114.48, 110.79, 63.19, 63.14, 62.94, 62.89, 48.00, 46.76, 40.49, 40.42, 40.32, 40.25, 40.16, 39.99, 39.82, 39.66, 39.49, 21.77, 20.77, 16.77, 16.73, 16.59, 16.54.ESI-HRMS *m/z* Calc for $C_{22}H_{27}N_2O_4P$ $[M-H]^-$:413.1681; found: 413.1681.

4b$_4$: Yield71.72%, ^{1}H NMR (500 MHz, DMSO) δ 11.89 (s, 1H), 8.03 (d, *J* = 3.7 Hz, 1H), 7.35 (s, 1H), 7.31 (d, *J* = 8.4 Hz, 1H), 7.22 (d, *J* = 8.4 Hz, 1H), 7.04 (dd, *J* = 8.4, 7.4 Hz, 2H), 6.71 (d, *J* = 7.8 Hz, 2H), 6.56 (t, *J* = 7.3 Hz, 1H), 6.32 (dd, *J* = 10.2, 6.3 Hz, 1H), 5.30 (dd, *J* = 24.4, 10.2 Hz, 1H), 4.13 – 3.86 (m, 4H), 2.31 (s, 3H), 1.27 – 1.24 (m, 1H), 1.22 (t, *J* = 7.0 Hz, 3H), 1.08 (t, *J* = 7.0 Hz, 3H).^{13}C NMR (126 MHz, DMSO) δ 161.56, 161.52, 147.45, 147.34, 137.53, 137.48, 136.47, 132.10, 131.65, 129.85, 129.34, 127.61, 119.35, 119.32, 117.76, 115.43, 113.67, 63.23, 63.18, 62.99, 62.93, 47.98, 46.73, 40.46, 40.38, 40.29, 40.21, 40.12, 40.05, 39.96, 39.79, 39.62, 39.46, 20.76, 16.76, 16.72, 16.57, 16.53.ESI-HRMS *m/z* Calc for $C_{21}H_{25}N_2O_4P$ $[M+Na]^+$:423.1450; found: 423.1451.

4b$_5$: Yield76.32%, ^{1}H NMR (400 MHz, DMSO) δ 12.05 (s, 1H), 8.06 (d, *J* = 3.4 Hz, 1H), 8.02 (d, *J* = 9.3 Hz, 2H), 7.96 (dd, *J* = 9.3, 5.6 Hz, 1H), 7.43 (s, 1H), 7.36 (d, *J* = 8.4 Hz, 1H), 7.25 (d, *J* = 8.4 Hz, 1H), 6.86 (d, *J* = 9.3 Hz, 2H), 5.47 (dd, *J* = 22.6, 9.4 Hz, 1H), 4.16 – 3.90 (m, 4H), 2.34 (s, 3H), 1.22 (t, *J* = 7.0 Hz, 3H), 1.11 (t, *J* = 7.0 Hz, 3H).^{13}C NMR (101 MHz, DMSO) δ 161.27, 161.21, 153.72, 153.61, 138.23, 138.17, 137.63, 136.63, 132.53, 131.85, 128.47, 127.81, 126.43, 119.14, 119.12, 115.55, 112.42, 63.42, 63.35, 63.29, 47.73, 46.18, 40.60, 40.39, 40.18, 39.97, 39.76, 39.56, 39.35, 20.77, 16.78, 16.73, 16.59, 16.54.ESI-HRMS *m/z* Calc for $C_{21}H_{24}N_3O_6P$ $[M-H]^-$:444.1344; found: 444.1357.

4b$_6$: Yield84.63%, ^{1}H NMR (400 MHz, DMSO) δ 11.98 (s, 1H), 8.03 (d, *J* = 3.5 Hz, 1H), 7.42 – 7.37 (m, 3H), 7.34 (d, *J* = 8.4 Hz, 1H), 7.24 (d, *J* = 8.4 Hz, 1H), 7.17 (dd, *J* = 9.7, 6.1 Hz, 1H), 6.85 (d, *J* = 8.7 Hz, 2H), 5.37 (dd, *J* = 23.7, 9.7 Hz, 1H), 4.16 – 3.88 (m, 4H), 2.33 (s, 3H), 1.22 (t, *J* = 7.0 Hz, 3H), 1.10 (t, *J* = 7.0 Hz, 3H).^{13}C NMR (101 MHz, DMSO) δ 161.42, 161.37, 150.79, 150.66, 137.80, 137.74, 136.55, 132.32, 131.74, 129.16, 127.70, 126.88, 126.73, 126.69, 124.20, 119.23, 119.20, 117.58, 117.27, 116.95, 115.49, 113.00, 63.31, 63.25, 63.16, 63.09, 47.66, 46.11, 40.60, 40.39, 40.18, 39.98, 39.77, 39.56, 39.35, 20.77, 16.77, 16.72, 16.59, 16.53.ESI-HRMS *m/z* Calc for $C_{21}H_{24}FN_2O_4P$ $[M+Na]^+$:441.1355; found: 441.1368.

4b$_7$: Yield59.59%, ^{1}H NMR (500 MHz, DMSO) δ 11.76 (s, 1H), 8.00 (d, *J* = 3.6 Hz, 1H), 7.25 (d, *J* = 8.9 Hz, 1H), 7.18 (d, *J* = 2.5 Hz, 1H), 7.14 (dd, *J* = 8.9, 2.6 Hz, 1H), 4.48 (d, *J* = 21.8 Hz, 1H), 4.13 – 4.05 (m, 2H), 3.94 – 3.85 (m, 2H), 3.79 (s, 3H), 2.49 – 2.31 (m, 2H), 1.35 (dd, *J* = 14.0, 7.0 Hz, 2H), 1.30 – 1.22 (m, 8H), 1.08 (t, *J* = 7.0 Hz, 3H), 0.83 (t, *J* = 7.2 Hz, 3H).^{13}C NMR (126 MHz, DMSO) δ 161.52, 161.47, 154.73, 137.33, 137.28, 132.91, 130.20, 120.11, 119.90, 116.69, 109.52, 62.91, 62.85, 62.44, 62.38, 55.93, 53.21, 51.97, 47.66, 47.54, 40.48, 40.41, 40.31, 40.24, 40.15, 39.98, 39.81, 39.65, 39.48, 31.85, 20.17, 16.79, 16.75, 16.64, 16.60, 14.27, 8.41.ESI-HRMS *m/z* Calc for $C_{22}H_{24}F_3N_2O_4P$ $[M+Na]^+$:491.1323; found: 491.1328.

4c$_1$: Yield59.59%, ^{1}H NMR (500 MHz, DMSO) δ 11.76 (s, 1H), 8.00 (d, *J* = 3.6 Hz, 1H), 7.25 (d, *J* = 8.9 Hz, 1H), 7.18 (d, *J* = 2.5 Hz, 1H), 7.14 (dd, *J* = 8.9, 2.6 Hz, 1H), 4.48 (d, *J* = 21.8 Hz, 1H), 4.13 – 4.05 (m, 2H), 3.94 – 3.85 (m, 2H), 3.79 (s, 3H), 2.49 – 2.31 (m, 2H), 1.35 (dd, *J* = 14.0, 7.0 Hz, 2H), 1.30 – 1.22 (m, 8H), 1.08 (t, *J* = 7.0 Hz, 3H), 0.83 (t, *J* = 7.2 Hz, 3H).^{13}C NMR (126 MHz, DMSO) δ 161.52, 161.47, 154.73, 137.33, 137.28, 132.91, 130.20, 120.11, 119.90, 116.69, 109.52, 62.91, 62.85, 62.44, 62.38, 55.93, 53.21, 51.97, 47.66, 47.54, 40.48, 40.41, 40.31, 40.24, 40.15, 39.98, 39.81, 39.65, 39.48, 31.85, 20.17, 16.79, 16.75, 16.64, 16.60, 14.27, 8.41.ESI-HRMS *m/z* Calc for $C_{19}H_{29}N_2O_5P$ $[M+H]^+$:397.1892; found: 397.1908.

4c$_2$: Yield79.27%, ^{1}H NMR (500 MHz, DMSO) δ 11.86 (s, 1H), 8.02 (d, *J* = 3.7 Hz, 1H), 7.25 (d, *J* = 9.0 Hz, 1H), 7.13 (dd, *J* = 8.9, 2.6 Hz, 1H), 7.07 (d, *J* = 2.7 Hz, 1H), 6.85 (d, *J* = 8.3 Hz, 2H), 6.61 (d, *J* = 8.5 Hz, 2H), 6.06 (dd, *J* = 10.1, 6.6 Hz, 1H), 5.26 (dd, *J* = 24.6, 10.2 Hz, 1H), 4.12 (dq, *J* = 14.2, 7.1 Hz, 2H), 4.01 – 3.86 (m, 2H), 3.76 (s, 3H), 2.09 (s, 3H), 1.23 (t, *J* = 7.0 Hz, 3H), 1.08 (t, *J* = 7.0 Hz, 3H).^{13}C NMR (126 MHz, DMSO) δ 161.22, 161.18, 154.78, 145.06, 144.94, 137.19, 137.14, 132.97, 130.46, 129.77, 126.28, 120.16, 119.96, 119.94, 116.83, 113.81, 109.33, 63.19, 63.14, 62.95, 62.90, 55.90, 48.33, 47.09, 40.50, 40.42, 40.33, 40.26, 40.17, 40.00, 39.83, 39.67, 39.50, 20.45, 16.77, 16.73, 16.59, 16.55.ESI-HRMS *m/z* Calc for $C_{22}H_{27}N_2O_5P$ $[M+H]^+$:431.1736; found: 431.1742.

4c$_3$: Yield74.36%, ^{1}H NMR (500 MHz, DMSO) δ 11.87 (s, 1H), 8.04 (d, *J* = 3.6 Hz, 1H), 7.25 (d, *J* = 8.9 Hz, 1H), 7.14 (dd, *J* = 8.9, 2.6 Hz, 1H), 7.09 (d, *J* = 2.7 Hz, 1H), 6.92 (t, *J* = 7.8 Hz, 1H), 6.56 (s, 1H), 6.48 (d, *J* = 8.1 Hz, 1H), 6.39 (d, *J* = 7.4 Hz, 1H), 6.17 (dd, *J* = 10.0, 6.5 Hz, 1H), 5.29 (dd, *J* = 24.5, 10.0 Hz, 1H), 4.11 (dq, *J* = 14.2, 7.1 Hz, 2H), 4.01 – 3.87 (m, 2H), 3.77 (s, 3H), 2.13 (s, 3H), 1.24 (dt, *J* = 14.1, 7.0 Hz, 4H), 1.09 (t, *J* = 7.0 Hz, 3H).^{13}C NMR (126 MHz, DMSO) δ 161.20, 161.16, 154.80, 147.39, 147.27, 138.35, 137.25, 137.20, 132.99, 130.46, 129.23, 120.20, 119.97, 118.67, 116.85, 114.44, 110.70, 109.36, 63.21, 63.16, 62.99, 62.93, 55.91, 48.03, 46.79, 40.48, 40.41, 40.32,

View Article Online
DOI: 10.1039/C7MD00098G

40.24, 40.15, 39.98, 39.82, 39.65, 39.48, 21.77, 16.77, 16.72, 16.59, 16.55.ESI-HRMS *m/z* Calc for $C_{22}H_{27}N_2O_5P$ $[M+Na]^+$:453.1555; found: 453.1574.

4c$_4$: Yield77%, ^{1}H NMR (500 MHz, DMSO) δ 11.88 (s, 1H), 8.04 (d, *J* = 3.6 Hz, 1H), 7.26 (d, *J* = 8.9 Hz, 1H), 7.14 (dd, *J* = 8.9, 2.7 Hz, 1H), 7.09 (d, *J* = 2.7 Hz, 1H), 7.05 (dd, *J* = 8.3, 7.5 Hz, 2H), 6.70 (d, *J* = 8.1 Hz, 2H), 6.57 (t, *J* = 7.3 Hz, 1H), 6.28 (dd, *J* = 9.9, 6.6 Hz, 1H), 5.30 (dd, *J* = 24.5, 10.0 Hz, 1H), 4.15 – 4.09 (m, 2H), 4.02 – 3.88 (m, 2H), 3.76 (s, 3H), 1.27 – 1.24 (m, 1H), 1.22 (t, *J* = 7.0 Hz, 3H), 1.09 (t, *J* = 7.0 Hz, 3H). ^{13}C NMR (126 MHz, DMSO) δ 161.21, 161.17, 154.81, 147.38, 147.27, 137.31, 137.26, 132.97, 130.30, 129.36, 120.24, 119.96, 119.94, 117.78, 116.88, 113.62, 109.36, 63.26, 63.20, 63.04, 62.98, 55.90, 48.03, 46.79, 40.44, 40.27, 40.11, 39.94, 39.77, 39.60, 39.44, 16.75, 16.71, 16.58, 16.53.ESI-HRMS *m/z* Calc for $C_{21}H_{25}N_2O_5P$ $[M+Na]^+$:439.1399; found: 439.1403.

4c$_5$: Yield80.08%, ^{1}H NMR (400 MHz, DMSO) δ 12.03 (s, 1H), 8.07 (d, *J* = 3.4 Hz, 1H), 8.02 (d, *J* = 9.3 Hz, 2H), 7.94 (dd, *J* = 9.1, 6.1 Hz, 1H), 7.29 (d, *J* = 8.8 Hz, 1H), 7.18 (dt, *J* = 8.1, 2.6 Hz, 2H), 6.85 (d, *J* = 9.2 Hz, 2H), 5.46 (dd, *J* = 22.7, 9.1 Hz, 1H), 4.18 – 3.93 (m, 4H), 3.79 (s, 3H), 1.22 (t, *J* = 7.0 Hz, 3H), 1.11 (t, *J* = 7.0 Hz, 3H).^{13}C NMR (101 MHz, DMSO) δ 160.91, 160.85, 154.89, 153.69, 153.58, 137.98, 137.93, 137.63, 133.13, 128.91, 126.43, 120.71, 119.76, 119.73, 117.00, 109.47, 63.43, 63.38, 63.31, 55.95, 47.82, 46.27, 40.60, 40.39, 40.18, 39.97, 39.77, 39.56, 39.35, 16.78, 16.72, 16.60, 16.55.ESI-HRMS *m/z* Calc for $C_{21}H_{24}N_3O_7P$ $[M+Na]^+$:484.1250; found: 484.1273.

4c$_6$: Yield86.00%, ^{1}H NMR (400 MHz, DMSO) δ 11.90 (s, 1H), 8.03 (d, *J* = 3.6 Hz, 1H), 7.26 (d, *J* = 9.0 Hz, 1H), 7.15 (dd, *J* = 8.9, 2.6 Hz, 1H), 7.09 (d, *J* = 2.6 Hz, 1H), 6.90 (t, *J* = 8.9 Hz, 2H), 6.74 – 6.66 (m, 2H), 6.33 (dd, *J* = 9.9, 6.7 Hz, 1H), 5.24 (dd, *J* = 24.4, 10.0 Hz, 1H), 4.15 – 3.84 (m, 4H), 3.77 (s, 3H), 1.23 (t, *J* = 7.0 Hz, 3H), 1.08 (t, *J* = 7.0 Hz, 3H).^{13}C NMR (101 MHz, DMSO) δ 161.21, 161.16, 156.64, 154.79, 154.33, 144.05, 143.90, 137.31, 137.25, 132.99, 130.14, 120.31, 119.90, 119.87, 116.88, 115.87, 115.65, 115.43, 115.06, 114.99, 114.53, 114.45, 109.28, 63.23, 63.17, 63.02, 62.95, 55.90, 48.57, 47.02, 40.61, 40.40, 40.19, 39.98, 39.77, 39.56, 39.35, 16.79, 16.74, 16.60, 16.54.ESI-HRMS *m/z* Calc for $C_{21}H_{24}FN_2O_5P$ $[M+Na]^+$:457.1305; found: 457.1323.

4c$_7$: Yield74.08%, ^{1}H NMR (400 MHz, DMSO) δ 11.96 (s, 1H), 8.04 (d, *J* = 3.6 Hz, 1H), 7.39 (d, *J* = 8.7 Hz, 2H), 7.27 (d, *J* = 8.9 Hz, 1H), 7.15 (ddd, *J* = 13.0, 7.7, 2.6 Hz, 3H), 6.84 (d, *J* = 8.6 Hz, 2H), 5.36 (dd, *J* = 23.8, 9.4 Hz, 1H), 4.15 – 3.89 (m, 4H), 3.78 (s, 3H), 1.22 (t, *J* = 7.0 Hz, 3H), 1.10 (t, *J* = 7.0 Hz, 3H).^{13}C NMR (101 MHz, DMSO) δ 161.06, 161.01, 154.84, 150.74, 150.61, 137.55, 137.49, 133.05, 129.59, 126.89, 126.70, 124.20, 120.49, 119.83, 119.80, 117.57, 117.25, 116.93, 112.96, 109.36, 63.32, 63.26, 63.19, 63.12, 55.91, 47.73, 46.18, 40.60, 40.39, 40.18, 39.97, 39.76, 39.56, 39.35, 16.77, 16.72, 16.60, 16.54.ESI-HRMS *m/z* Calc for $C_{21}H_{24}F_3N_2O_5P$ $[M+Na]^+$:507.1273; found: 507.1252.

4d$_1$: Yield43.26%, ^{1}H NMR (400 MHz, DMSO) δ 11.80 (s, 1H), 7.92 (d, *J* = 3.4 Hz, 1H), 7.17 (s, 1H), 6.83 (s, 1H), 6.10 (s, 2H), 4.44 (d, *J* = 21.4 Hz, 1H), 4.08 (ddd, *J* = 10.2, 8.7, 5.3 Hz, 2H), 3.97 – 3.82 (m, 2H), 2.50 – 2.34 (m, 2H), 1.40 – 1.22 (m, 10H), 1.08 (t, *J* = 7.0 Hz, 3H), 0.83 (t, *J* = 7.2 Hz, 3H).^{13}C NMR (101 MHz, DMSO) δ 174.78, 161.75, 161.69, 150.38, 143.78, 137.65, 137.58, 135.35, 130.11, 126.35, 113.81, 113.78, 105.58, 102.20, 95.38, 62.85, 62.78, 62.41, 62.34, 53.17, 51.62, 47.63, 47.47, 31.78, 30.84, 29.56, 29.51, 29.46, 29.31, 29.18, 29.06, 27.02, 25.59, 22.58, 20.18, 16.82, 16.77, 16.66, 16.61, 14.42, 14.30.ESI-HRMS *m/z* Calc for $C_{19}H_{27}N_2O_6P$ $[M+H]^+$:411.1585; found: 411.1519.

4d$_2$: Yield66.81%, ^{1}H NMR (500 MHz, DMSO) δ 11.85 (s, 1H), 7.92 (d, *J* = 3.5 Hz, 1H), 7.08 (s, 1H), 6.85 (d, *J* = 8.3 Hz, 2H), 6.82 (s, 1H), 6.60 (d, *J* = 8.5 Hz, 2H), 6.07 (s, 2H), 6.02 (dd, *J* = 10.1, 6.5 Hz, 1H), 5.20 (dd, *J* = 24.3, 10.1 Hz, 1H), 4.10 (dq, *J* = 14.2, 7.1 Hz, 2H), 4.01 – 3.83 (m, 2H), 2.09 (s, 3H), 1.22 (t, *J* = 7.1 Hz, 3H), 1.08 (t, *J* = 7.0 Hz, 3H).^{13}C NMR (126 MHz, DMSO) δ 161.44, 161.40, 150.49, 145.13, 145.01, 143.88, 137.47, 137.42, 135.47, 129.74, 126.68, 126.18, 113.79, 113.70, 113.68, 105.44, 102.22, 95.45, 63.10, 63.05, 62.89, 62.83, 48.14, 46.90, 40.49, 40.42, 40.33, 40.25, 40.16, 39.99, 39.83, 39.66, 39.49, 20.45, 16.77, 16.72, 16.59, 16.54.ESI-HRMS *m/z* Calc for $C_{22}H_{25}N_2O_6P$ $[M+Na]^+$:467.1348; found: 467.1381.

4d$_3$: Yield77.29%, ^{1}H NMR (400 MHz, DMSO) δ 11.94 (s, 1H), 7.95 (d, *J* = 3.3 Hz, 1H), 7.10 (s, 1H), 6.89 (dd, *J* = 15.8, 7.0 Hz, 3H), 6.70 (dd, *J* = 8.9, 4.5 Hz, 2H), 6.30 (dd, *J* = 9.8, 6.6 Hz, 1H), 6.08 (s, 2H), 5.19 (dd, *J* = 24.2, 10.0 Hz, 1H), 4.16 – 4.06 (m, 2H), 3.94 (ddt, *J* = 25.1, 10.0, 7.5 Hz, 2H), 3.06 (d, *J* = 7.2 Hz, 1H), 1.21 (q, *J* = 7.2 Hz, 6H), 1.09 (t, *J* = 7.0 Hz, 3H).^{13}C NMR (101 MHz, DMSO) δ 161.46, 161.41, 156.62, 154.31, 150.58, 144.14, 143.98, 143.94, 137.63, 137.57, 135.54, 130.11, 126.31, 115.84, 115.63, 114.53, 114.46, 113.69, 113.66, 105.47, 102.28, 95.51, 63.18, 63.12, 62.99, 62.92, 48.40, 46.84, 45.82, 40.56, 40.35, 40.14, 39.93, 39.73, 39.52, 39.31, 35.59, 31.75, 30.84, 29.45, 29.17, 29.04, 27.01, 25.60, 22.57, 16.78, 16.73, 16.60, 16.54, 14.41, 8.89.ESI-HRMS *m/z* Calc for $C_{22}H_{25}N_2O_6P$ $[M-H]^-$:443.1372; found: 443.1727.

4d$_4$: Yield77.32%, ^{1}HNMR (500 MHz, DMSO) δ 11.87 (s, 1H), 7.94 (d, *J* = 3.4 Hz, 1H), 7.09 (s, 1H), 7.04 (dd, *J* = 8.3, 7.5 Hz, 2H), 6.82 (s, 1H), 6.70 (d, *J* = 7.8 Hz, 2H), 6.56 (t, *J* = 7.3 Hz, 1H), 6.25 (dd, *J* = 9.9, 6.6 Hz, 1H), 6.07 (s, 2H), 5.23 (dd, *J* = 24.2, 9.9 Hz, 1H), 4.10 (dq, *J* = 14.2, 7.1 Hz, 2H), 4.02 – 3.84 (m, 2H), 1.22 (t, *J* = 7.1 Hz, 3H), 1.08 (t, *J* = 7.0 Hz, 3H).^{13}C NMR (126 MHz, DMSO) δ 161.43, 161.38, 150.54, 147.49, 147.38, 143.92, 137.56, 137.52, 135.52, 129.32, 126.57, 117.65, 113.70, 113.68, 113.59, 105.48, 102.25, 95.48, 63.13, 63.08, 62.95, 62.89, 47.83, 46.58, 40.49, 40.42, 40.33, 40.25, 40.16, 39.99, 39.82, 39.66, 39.49, 16.76, 16.72, 16.59, 16.54.ESI-HRMS *m/z* Calc for $C_{21}H_{23}N_2O_6P$ $[M+Na]^+$:453.1191; found: 453.1169.

4d$_5$: Yield73.71%, ^{1}H NMR (400 MHz, DMSO) δ 12.02 (s, 1H), 8.08 – 7.93 (m, 4H), 7.18 (s, 1H), 6.84 (s, 3H), 6.10 (s, 2H), 5.40 (dd, *J* = 22.4, 9.2 Hz, 1H), 4.13 – 3.91 (m, 4H), 1.20 (t, *J* = 7.0 Hz, 3H), 1.11 (t, *J* = 7.0 Hz, 3H). ^{13}C NMR (101 MHz, DMSO) δ 161.16, 161.10, 153.75, 153.65, 150.89, 144.09, 138.24, 138.18, 137.54, 136.93, 135.78, 126.44, 125.10, 113.55, 113.52, 112.29, 105.67, 102.38, 95.51, 63.34, 63.32, 63.28, 63.25, 47.62, 46.06, 40.59, 40.38, 40.17, 39.97, 39.76, 39.55, 39.34, 16.78, 16.72, 16.60, 16.54, -14.99.ESI-HRMS *m/z* Calc for $C_{21}H_{22}N_3O_8P$ $[M+Na]^+$:498.1042; found: 498.1064.

4d$_6$: Yield85.70%, ^{1}H NMR (400 MHz, DMSO) δ 11.98 (s,1H), 7.94 (d, *J* = 3.2 Hz,1H), 7.38 (d, *J* = 8.6 Hz,2H), 7.15 – 7.06

View Article Online
DOI: 10.1039/C7MD00098G

(m,2H), 6.88 – 6.79 (m,3H), 6.08 (s,2H), 5.29 (dd, *J* = 23.5, 9.4 Hz,1H), 4.13 – 4.07 (m,2H), 4.02 – 3.86 (m,3H), 1.26 – 1.18 (m,6H), 1.09 (t, *J* = 7.0 Hz,3H).^{13}C NMR (101 MHz, DMSO) δ 161.32, 150.72, 144.01, 137.81, 135.65, 126.71, 125.77, 113.63, 112.94, 105.56, 102.32, 95.52, 63.27, 63.20, 63.15, 63.08, 47.54, 45.97, 40.54, 40.33, 40.12, 39.91, 39.70, 39.50, 39.29, 29.02, 22.56, 16.76, 16.71, 16.59, 16.53.ESI-HRMS *m/z* Calc for $C_{21}H_{22}FN_2O_6P$ $[M+Na]^+$:471.1097; found: 471.1118.

4d$_7$: Yield75.49%, ^{1}H NMR (400 MHz, DMSO) δ 11.94 (s, 1H), 7.95 (d, *J* = 3.3 Hz, 1H), 7.10 (s, 1H), 6.89 (dd, *J* = 15.8, 7.0 Hz, 3H), 6.70 (dd, *J* = 8.9, 4.5 Hz, 2H), 6.30 (dd, *J* = 9.8, 6.6 Hz, 1H), 6.08 (s, 2H), 5.19 (dd, *J* = 24.2, 10.0 Hz, 1H), 4.17 – 4.06 (m, 2H), 4.03 – 3.83 (m, 2H), 3.06 (d, *J* = 7.2 Hz, 1H), 1.21 (q, *J* = 7.2 Hz, 6H). ^{13}C NMR (101 MHz, DMSO) δ 161.03 (d, *J* = 5.4 Hz), 154.84 (s), 150.68 (d, *J* = 12.7 Hz), 137.52 (d, *J* = 6.0 Hz), 133.05 (s), 129.59 (s), 126.79 (d, *J* = 19.3 Hz), 120.49 (s), 119.82 (d, *J* = 3.1 Hz), 117.57 (s), 117.25 (s), 116.93 (s), 112.96 (s), 109.36 (s), 63.22 (dd, *J* = 14.0, 6.9 Hz), 55.91 (s), 47.73 (s), 46.18 (s), 40.60 (s), 40.39 (s), 40.18 (s), 39.97 (s), 39.76 (s), 39.56 (s), 39.35 (s), 16.66 (dd, *J* = 17.6, 5.4 Hz).ESI-HRMS *m/z* Calc for $C_{22}H_{22}F_3N_2O_6P$ $[M+Na]^+$:521.1065; found: 521.1089.

3.1.2 General procedure for compound 5(5a-5d)

2-oxo-quinoline 3-carbaldehyde derivatives **3** (1 mmol), diethyl 4-aminobenzylphosphonate (1.5 mmol) and 5 mL toluene were mixed in pressure tube and reacted at 120^{o}C for 4h. After the reaction, the mixture was cooled to room temperature and filtered to yield compound **5** as pale yellow powder.

5a: Yield70.81%, ^{1}H NMR (400 MHz, DMSO) δ 11.68 (s, 1H), 7.72 (d, J = 2.6 Hz, 1H), 6.86 (s, 1H), 6.69 (t, J = 7.7 Hz, 1H), 6.60 (s, 1H), 6.33 (s, 1H), 6.26 (d, J = 8.0 Hz, 1H), 6.16 (d, J = 7.3 Hz, 1H), 5.98 – 5.90 (m, 1H), 5.85 (s, 2H), 5.01 (dd, J = 24.2, 10.0 Hz, 1H), 3.93 – 3.82 (m, 2H), 3.79 – 3.62 (m, 2H), 1.91 (s, 3H), 0.99 (t, J = 7.0 Hz, 3H), 0.86 (t, J = 7.0 Hz, 3H).^{13}C NMR (101 MHz, DMSO) δ 161.44, 161.38, 150.52, 147.49, 147.35, 143.91, 138.31, 137.56, 137.49, 135.49, 129.20, 126.69, 118.57, 114.40, 113.71, 113.68, 110.68, 105.46, 102.25, 95.46, 63.14, 63.08, 62.94, 62.87, 47.92, 46.36, 46.03, 21.78, 16.78, 16.73, 16.60, 16.54.ESI-HRMS *m/z* Calc for $C_{21}H_{23}N_2O_4P$ $[M+H]^+$:399.1474; found: 339.1476.

5b: Yield63.13%, ^{1}H NMR (400 MHz, DMSO) δ 12.10 (s, 1H), 8.79 (s, 1H), 8.59 (s, 1H), 7.67 (s, 1H), 7.42 (dd, *J* = 8.4, 1.7 Hz, 1H), 7.34 (dd, *J* = 8.5, 2.3 Hz, 2H), 7.25 (dd, *J* = 12.0, 8.3 Hz, 3H), 3.97 (dq, *J* = 14.2, 7.1 Hz, 4H), 3.27 (d, *J* = 21.5 Hz, 2H), 2.36 (s, 3H), 1.19 (t, *J* = 7.0 Hz, 6H).^{13}C NMR (101 MHz, DMSO) δ 161.91, 155.52, 150.44, 150.40, 138.36, 137.77, 133.82, 131.91, 131.19, 131.13, 130.97, 130.88, 129.41, 126.80, 121.47, 121.44, 119.29, 115.60, 61.90, 61.84, 40.60, 40.40, 40.19, 39.98, 39.77, 39.56, 39.35, 32.93, 31.59, 20.87, 16.72, 16.66. ESI-HRMS *m/z* Calc for $C_{22}H_{25}N_2O_4P$ $[M-H]^-$: 411.1474; found: 411.1549.

5c: Yield64.65%, ^{1}H NMR (500 MHz, DMSO) δ 12.06 (s, 1H), 8.80 (s, 1H), 8.64 (s, 1H), 7.46 (d, *J* = 2.7 Hz, 1H), 7.34 (dd, *J* = 8.4, 2.3 Hz, 2H), 7.30 (d, *J* = 8.9 Hz, 1H), 7.24 (dd, *J* = 8.9, 2.8 Hz, 3H), 3.96 (dd, *J* = 15.1, 7.1 Hz, 4H), 3.26 (d, *J* = 21.5 Hz, 2H), 1.18 (t, *J* = 7.0 Hz, 6H).^{13}C NMR (126 MHz, DMSO) δ 190.33, 161.58, 155.45, 154.95, 150.38, 150.35, 137.62, 135.01, 131.19, 131.14, 131.02, 130.94, 127.13, 122.03, 121.45, 121.43, 119.94, 116.98, 110.97, 61.90, 61.85, 55.99, 40.52, 40.45, 40.36, 40.28, 40.19, 40.02, 39.85, 39.69, 39.52, 32.85, 31.78, 16.70, 16.66.ESI-HRMS *m/z* Calc for $C_{22}H_{25}N_2O_5P$ $[M+Na]^+$: 451.1399; found: 451.1404.

5d: Yield70.98%, ^{1}H NMR (400 MHz, *d*-DMSO) δ 12.08 (s, 1H), 8.74 (s, 1H), 8.56 (s, 1H), 7.38 (d, J = 8.7 Hz, 2H), 7.32 (dd, J = 8.4, 2.3 Hz, 2H), 7.20 (d, J = 8.0 Hz, 2H), 6.15 (d, J = 8.2 Hz, 2H), 3.97 (dd, J = 8.0, 7.2 Hz, 4H), 3.26 (d, J = 21.5 Hz, 2H), 1.19 (t, J = 7.0 Hz, 6H). ^{13}C NMR (101 MHz, DMSO) δ 189.85, 161.90, 155.37, 153.66, 152.08, 144.53, 142.07, 140.40, 131.17, 122.90, 121.34, 113.87, 113.23, 107.29, 106.73, 103.01, 102.65, 95.37, 61.83, 32.81, 31.44, 16.71.ESI-HRMS *m/z* Calc for $C_{22}H_{23}N_2O_6P$ $[M+H]^+$: 443.1372; found: 443.1391.

3.2. Biological Assays

The detailed procedures for other experimental methods are described in the Supplementary data (Part 2). The materials, instrumentation, and methods for the cytotoxicity assay, cell cycle analysis, cell apoptosis analysis, western blot and transfection assays were described in our previous work.[26]

4. Conclusions

In summary, we have designed and synthesized a set of 2-oxo quinoline APA derivatives (**4-5**) and evaluated the cytotoxicity of target compounds on three cancer cell lines (HepG2, SKOV-3 and NCI-H460). The target compounds displayed evident anticancer activity with low cytotoxicity against normal HL-7702 cells. The cell apoptosis-inducing investigation of representative compound **5b** in HpeG2 cells showed that antitumor activity of this compound may rely on the apoptosis of cancer cells by regulation of levels of Bax, Bcl-2 and cytochrome *c*, intracellular Ca^{2+} release and ROS generation, activation of caspase-9 and caspase-3 and subsequent cleavage of PARP. Cell cycle study revealed that antitumor activity of compound **5b** might be exerted by G_2/M phase arrest that accompanied by the expression of p53, p21 and p27 proteins. The above results confirmed that the rational design of 2-oxo-quinoline APA derivatives as novel antitumor agents was feasible.

Acknowledgements

This study was supported by the National Natural Science Foundation of China (No. 21501032), Guangxi Natural Science Foundation of China (Nos. 2016GXNSFAA380300 and 2014GXNSFBA118050) and State Key Laboratory Cultivation Base for the Chemistry and Molecular Engineering of Medicinal Resources，Ministry of Science and Technology of China (No. CMEMR2014-B14).

Notes and references

1 S. Raghavana, P. Manogaranb, K. K. Gadepalli Narasimha, B. K. Kuppusamia, P. Mariyappana, A.

View Article Online
DOI: 10.1039/C7MD00098G

Gopalakrishnanb and G. Venkatraman, *Bioorg. Med. Chem. Lett.*, 2015, **25**, 3601.
2 R. Abonia, D. Insuasty, J. Castillo, B. Insuasty, J. Quiroga, M. Nogueras and J. Cobo, *Eur. J. Med. Chem*., 2012, **57**, 29.
3 Y. Zhang, Y. L. Fang, H. Liang, H. S. Wang, K. Hu, X. X. Liu, X. H. Yi and Y. Peng, *Bioorg. Med. Chem. Lett.*, 2013, **23**, 107.
4 Y. Zhang, X. H. Yi, Y. L. Fang, X. X. Liu, *patent(in China)*, ZL.201210407465X.
5 Y. K. Tyagi, A. Kumar, H. G. Raj, P. Vohra, G. Gupta, R. Kumari, P. Kumar and R. K. Gupta, *Eur. J. Med. Chem*., 2005, **40**, 413.
6 R. V. Patel, B. Mistry, R. Syed, A. K. Rathi, Y. J. Lee, J. S. Sung, H. S. Shinf and Y. S. Keum, *Eur. J. Pharm. Sci.*, 2016, **88**, 166.
7 O. Vang and D. K. Das, Resveratrol and health, New York Academy of Sciences, 2011.
8 X. L. Tang, X. Y. Yang, H. J. Jung, S. Y. Kim, S. Y. Jung, D. Y. Choi, W. C. Park and H. Park, *Biol. Pharm. Bull.*, 2009, **32**, 1399.
9 J. A. Kim, Y. S. Lee, D. Q. Jin, E. J. Kwon, S. H. Park, E. S. Lee, T. C. Jeong and D. H. Nam, *Cancer Lett.*, 2002, **186**, 83.
10 Y. L. Fang, Z. L. Wu, M. W. Xiao, Y. T. Tang, K. M. Li, J. Ye, J. N. Xiang, A. X. Hu, *Int. J. Mol. Sci*., 2016, **17**, 653.
11 J. A. Choi, J. Y. Kim, J. Y. Lee, C. M. Kang, H. J. Kwon, Y. D. Yoo, T. W. Kim, Y. S. Lee, and S. J. Lee, *Int. J. Oncol.*, 2001, **19**, 837.
12 M. B. Kastan and J. Bartek, *Nature*, 2004, **432**, 316.
13 S. U. Dighe, S. Khan, I. Soni, P. Jain, S. Shukla, R. Yadav, P. Sen, S. M. Meeran and S. Batra, *J. Med. Chem.*, 2015, **58**, 3485.
14 R. Boutros, V. Lobjois and B. Ducommun, *Nat. Rev. Cancer*, 2007, **7**, 495.
15 F. Belluti, G. Fontana, L. D. Bo, N. Carenini, C. Giommarelli and F. Zunino, *Bioorg. Med. Chem.*, 2010, **18**, 3543.
16 M.O. Hengartner, *Nature*, 2000, **407**, 770.
17 M. Y. Ye, G. Y. Yao, Y. M. Pan, Z. X. Liao, Y. Zhang and H. S. Wang, *Eur. J. Med. Chem*., 2014, **83**, 116..
18 R. Z. Huang, C. Y. Wang, J. F. Li, G. Y. Yao, Y. M. Pan, M. Y. Ye, H. S. Wang, and Y. Zhang, *RSC Advances*, 2016, **6**, 62890.
19 S. X. Hua, R. Z. Huang, M. Y. Ye, Y. M. Pan, G. Y. Yao, Y. Zhang and H. S. Wang, *Eur. J. Med. Chem*., 2015, **95**, 435.
20 R. Martin, J. Carvalho, E. Ibeas, M. Hernández, V. Ruiz-Gutierrez and M. Luisa-Nieto *Cancer Res*., 2007, **67**, 3741.
21 J. Neuzil, X. F. Wang, L. F. Dong, P. Low and S. J. Ralph, *FEBS Lett.*, 2006, **580**, 5125.
22 B. Yun, H. Lee, M. Ghosh, B. F. Cravatt, K. L. Hsu, J. V. Bonventre, H. Ewing, M. H. Gelb and C. C. Leslie, *J. Biol. Chem.*, 2014, **289**, 1491.
23 L. Gomez, P. A. Thiebaut, M. Paillard, S. Ducreux, M. Abrial, C. C. D. Silva, A. Durand, M. R. Alam, F. V. Coppenolle, S. S. Sheu and M. Ovize, *Cell Death Differ.*, 2016, **23**, 313.
24 S. Ghavami, M. Hashemi, S. R. Ande, B. Yeganeh, W. Xiao, M. Eshraghi, C. J. Bus, K. Kadkhoda, E. Wiechec, A. J. Halayko and M. Los, *J. Med. Genet.*, 2009, **46**: 497.
25 M. Chen and J. Wang, *Apoptosis*, 2002, **7**, 313.
26 J. F. Li，R. Z. Huang，G. Y. Yao，M. Y. Ye，H. S. Wang, Y. M. Pan and J. T. Xiao, *Eur. J. Med. Chem*., 2014, **86**, 175.

View Article Online
DOI: 10.1039/C7MD00098G

Graphical abstract

Design, synthesis and pharmacological evaluation of new 2-oxo-quinoline derivatives containing α-aminophosphonates as potential antitumor agents

Yan-Cheng Yu, Wen-Bin Kuang, Ri-Zhen Huang, Yi-Lin Fang, Ye Zhang, Zhen-Feng Chen, Xian-Li Ma

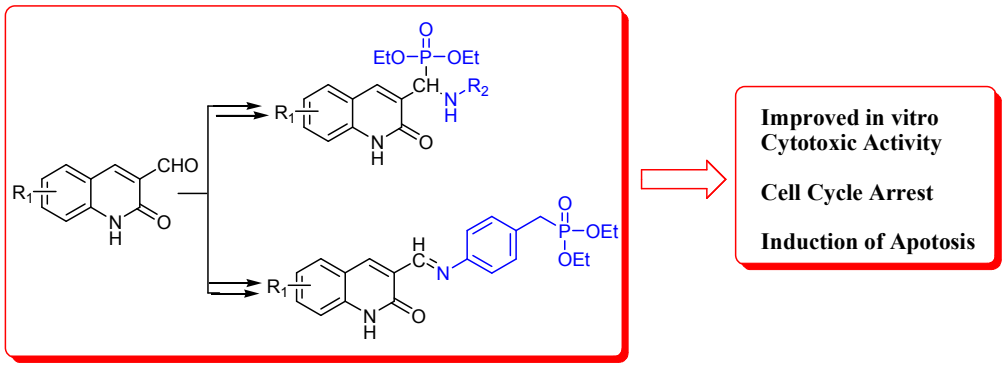

A series of novel 2-oxo-quinoline derivatives containing α-aminophosphonates was designed and synthesized as antitumor agents. Representative compound **5b** blocked the HepG2 cell cycle at G_2/M phase by the regulation of p53, p21 and p27 proteins and induced apoptosis through mitochondrial pathway.